Hindawi
Geofluids
Volume 2022, Article ID 8163011, 19 pages
https://doi.org/10.1155/2022/8163011

Research Article

Controlling Effect of Wave-Dominated Delta Sedimentary Facies on Unconventional Reservoirs: A Case Study of Pinghu Tectonic Belt in Xihu Sag, East China Sea Basin

Qinglong Chen,[1] **Renhai Pu**,[1] **Xiaomin Xue**,[2] **Ming Han**,[3] **Yanxin Wang**,[4] **Xin Cheng**,[1] **and Hanning Wu**[1]

[1]*State Key Laboratory of Continental Dynamics, Department of Geology, Northwest University, Xi'an 710069, China*
[2]*Gas Field Development Department, Petro China Changqing Oilfield Company, Xi'an 710018, China*
[3]*No.8 Oil Production Plant, Petro China Changqing Oilfield Company, CNPC, Xi'an 710021, China*
[4]*Exploration and Development Research Institute, Petro China Changqing Oilfield Company, Xi'an 710018, China*

Correspondence should be addressed to Qinglong Chen; chenqinglong@stumail.nwu.edu.cn
and Hanning Wu; wuhn2506@nwu.edu.cn

Received 12 March 2022; Accepted 9 May 2022; Published 11 June 2022

Academic Editor: Jin Qian

In order to find the "sweet spots" of unconventional oil and gas from the Pinghu Formation in the Pinghu Tectonic Belt, we are committed to clarifying the development and distribution rules of coal-measure source rocks and tight reservoirs as well as the controlling factors. Using 3D seismic and logging data, combined with logging constraints of target lithology and pyrolysis experiments of source rock, "source and reservoir" research of uncoventional oil and gas was carried out in the Pinghu Tectonic Belt. The results show that two stages of regression and one stage of transgression occurred in the Pinghu Formation, resulting in river-controlled and wave-controlled delta-neritic facies dominated by sedimentary facies, source rocks developed in interdistributary bay and swamp microfacies, and tight sandstones in point bar and distributary channel microfacies are developed. The accumulation of coalbed methane and shale gas is controlled by the sedimentary facies and the degree of thermal evolution under the factors of burial depth. The accumulation of tight sandstone is closely related to the dominantly sedimentary facies and diagenetic modification of physical properties and faults. It is concluded that the structural type, type and distribution of faults, and depositional environment of the Pinghu Tectonic Belt in the Xihu Sag are the key factors controlling the development and accumulation of coal-measure source rocks and tight sandstone reservoirs. This understanding provides a clear direction for the deep exploration of unconventional oil and gas in the sag and provides a reference for finding reservoir "sweet spots."

1. Introduction

Since the 21st century, the successful exploration and exploitation of shale gas represents the rapid development of unconventional oil and gas, and the world's oil and gas development has shifted from conventional oil and gas to unconventional oil and gas. China's tight oil and gas, shale oil and gas, coalbed methane and other unconventional oil, and gas resources are abundant and widely distributed [1], but China's unconventional oil and gas is still in the development stage. In recent years, some unconventional exploration achievements have been mainly concentrated on land, such as the Middle Permian tight sandstone gas reservoir in the Sulige Gas Field of the Ordos Basin [2] and the Permian Lucaogou Formation tight sandstone oil reservoir in the Junggar Basin. The exploration and development of offshore unconventional oil and gas are relatively weak, and the main exploration is concentrated in the Mesozoic tight oil reservoirs in the North Yellow Sea Basin, the Upper Paleozoic tight gas reservoirs in the South Yellow Sea Basin [3], and

the tight sandstone gas reservoirs in the Xihu Sag of the East China Sea [4]. The Xihu Sag is the largest hydrocarbon-rich sag in the offshore China, and its oil and gas reservoirs have great economic value. The discovered low permeability-tight sandstone reservoirs are rich in natural gas and condensate oil and gas [5], and coalbed methane and shale gas are also widely derived from coal-measure source rocks in the Pinghu Formation [6].

In China, sandstone reservoirs with porosity less than 12% and permeability less than 5 mD [7] are defined as tight sandstone reservoirs. The physical properties of the main reservoir as the Pinghu Formation in the Xihu Sag fully satisfy the standard of tight reservoir, and the oil and gas mainly accumulate in the overpressure surface, which is in line with the characteristics of tight sandstone oil and gas reservoirs [8]. These characteristics indicate that there are abundant tight oil and gas resources in the Xihu Sag. At the same time, coal-measure source rocks are widely developed and distributed in the Pinghu Formation, which can be divided into three types: carbonaceous mudstone, coal seam, and dark mudstone according to their hydrocarbon generation potential. According to organic geochemical analysis, it is believed that the kerogen types are mainly type II and type III, and most of them are in the mature stage. The average TOC distribution of dark mudstone is about 1%, the average TOC of carbonaceous mudstone is about 10%, and the TOC of coal seam in the Pinghu Formation is about 40% [9], of which has high abundance of organic matter, great possibility of hydrocarbon generation, and high economic development value. In spite of this, the current oil and gas exploration and development in the Xihu Sag are still dominated by conventional oil and gas, and unconventional oil and gas are still in the research stage. The slow progress in the exploration of three types unconventional oil and gas reservoirs, including coalbed methane, shale gas, and tight sandstone oil and gas, is mainly due to the key scientific issues that have not been effectively resolved, such as "sweet spot distribution" and "reservoir controlling factors." The conventional low permeability-tight composite strong heterogeneous physical properties in the sandstone reservoirs of the Pinghu Formation result in a distinct distribution of reservoir quality differences [10, 11], which restricts the search for "sweet spots" in high-quality reservoirs. Different scholars have explored the main controlling factors of low permeability-tight sandstone based on the depositional environment, diagenesis, and tectonic evolution. Many tight oil and gas accumulation studies believe that sediment provenance and dominant sedimentary facies are the primary factors determining the formation of high-quality reservoir "sweet spots" in the later stage; abnormal high pressure, oil and gas charging, and diagenesis play a role in the heterogeneity of reservoir quality. Therefore, for low permeability-tight sandstone reservoirs with large burial depth and quality differences in different layers, the exact distribution of its "sweet spots" needs to be studied in detail. As the main hydrocarbon-generating strata, the Pinghu Formation has the potential to generate coalbed methane and shale gas in theory. However, the horizontal and vertical distribution law of carbonaceous mudstone, coal seam, and dark mudstone and the controlling factors affecting their development and preservation are not yet clear, especially whether the sedimentary facies, tectonic faults, and paleo-topography have an impact on their distribution, and quantity variation depends on the above three is still to be resolved.

Based on the complex and diverse geological conditions of the Xihu Sag, in order to achieve the exploration goal of finding the "sweet spots" of high-quality reservoirs, it is impossible to effectively predict these unconventional oil and gas sweet spots by only relying on a single method. Therefore, the author studies the sedimentary facies and source rocks of the Pinghu Formation in the Pinghu Tectonic Belt. The combination of seismic, logging, and organic geochemistry research methods is used to clarify the main controlling factors of the delta facies and sedimentary evolution model of the Pinghu Formation, the logging response characteristics of coal-measure source rocks, and the level of organic matter content. In this way, the distribution law and controlling factors of source rocks can be clarified, and then, the distribution "sweet spots" of shale gas, coalbed methane, and tight sandstone reservoirs can be effectively predicted, and the favorable areas for unconventional oil and gas exploration in the Pinghu Formation of the slope belt are verified by combining the gas-bearing attenuation method. In this paper, the distribution thickness of coal-measure source rock is quantitatively calculated based on the logging response of coal measures, and the unconventional reservoir sweet spots are predicted by thickness inversion of sand reservoir and gas detection method based on seismic wave attenuation, which has certain innovation and practical value.

2. Geological Setting

The Xihu Sag is the largest Cenozoic hydrocarbon-bearing sag in the East China Sea shelf basin, with a total area of about 52,000 km^2, surrounded by many depressions and uplifts. Its tectonic formation and evolution were affected by the several geological movements of the Chinese continental plate, the Philippine plate, and the Pacific plate and experienced extensional rifting, fault-depression transformation, and tectonic inversion [12]. The tectonic framework is mainly characterized by "banded shape from east to west, block distribution from north to south," and from west to east is the Western Slope Belts, the Central Anticlinal Belts, and the Eastern Slope belts [13]. The study area is located in the Pinghu Tectonic Belt [14–16] in the west of the Xihu Sag (Figure 1(a)), which can be further divided into four structural units: the Pingbei gentle slope belt, the Pingzhong steep slope belt, the Pingnan gentle slope belt, and two transition belts. The seismic response reflects that the characteristics of the rifted basins are different. The basins under the large faults in the central and southern regions have more intense sedimentary sags, and there are obvious cliff-like sedimentary collapses. At the same time, the development of faults is complex, the faults are dense and deep, and they are basically broken from the basement to T30 (Figures 1(c)–1(f)).

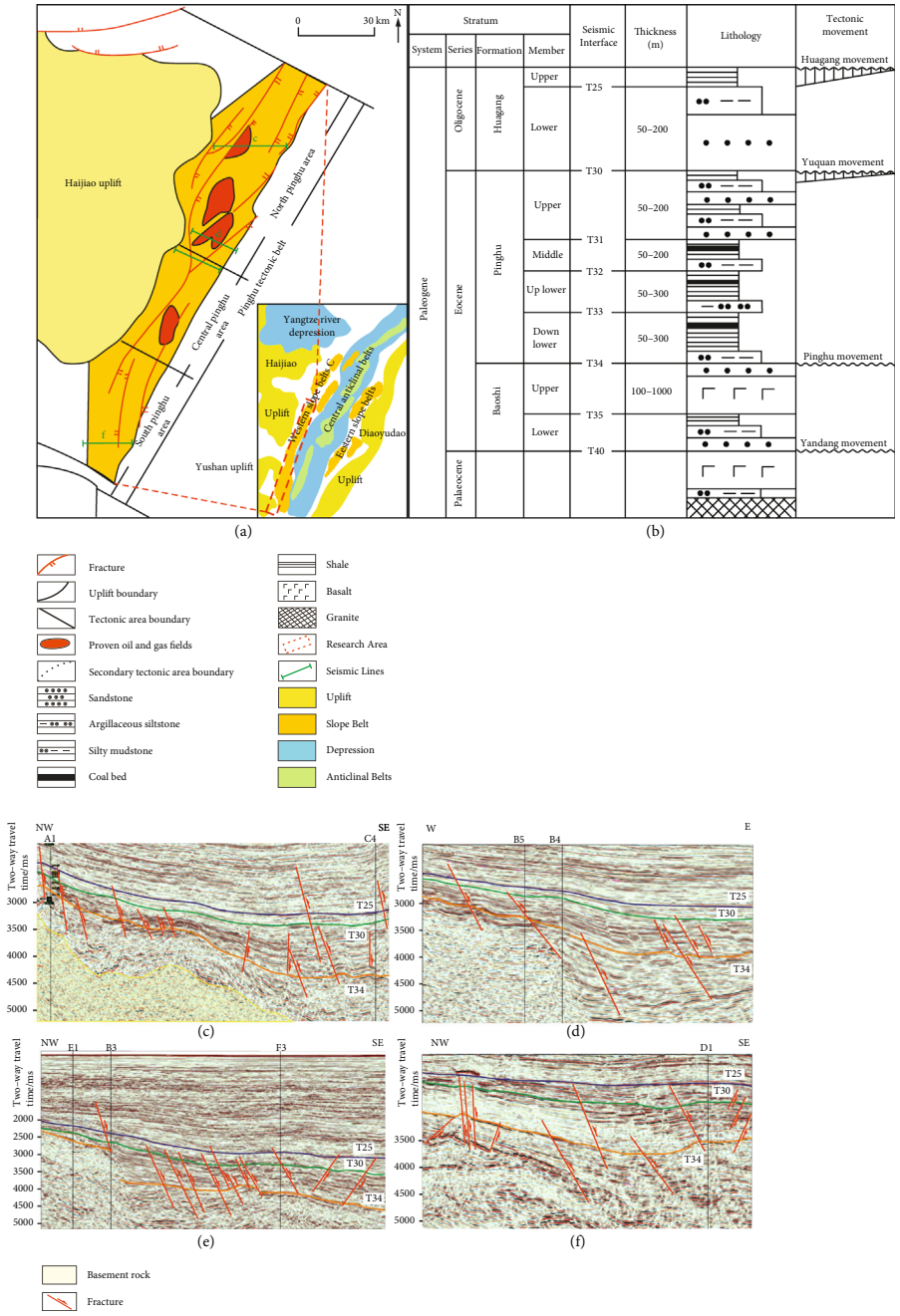

Figure 1: Tectonic development and stratigraphic columnar section of Pinghu Tectonic Belt in Xihu Sag (modified after Jiang et al. [17]): (a) study area and surrounding tectonic units; (b) stratigraphic age and lithology; (c) structural section and fault development in North Pinghu area; (d, e) structural section and fault development in Middle Pinghu area; (f) structural section and fault development in South Pinghu area.

The main target layers for oil and gas exploration in the study area are the Oligocene Huagang Formation and the Eocene Pinghu Formation, and the depositional development of the two is mainly tide-controlled, river-controlled, and wave-controlled delta facies in the coastal-neritic environment. The lithologic composition is dominated by interbeds of gray-black mudstone and sandstone, among which coal seams are mixed, and the cumulative thickness of the coal seams is about 500 m (Figure 1(b)). It is a good hydrocarbon-generating and hydrocarbon-storing interval with the characteristics of "self-generation and self-accumulation." At present, the oil and gas production in the Xihu Sag mainly derives from conventional oil and gas, and the accumulation types include anticline, faulted anticline, and fault block oil and gas reservoirs.

3. Samples and Methods

3.1. Sample Collection and Experimentation. The source rocks used in the source rock pyrolysis experiment for the

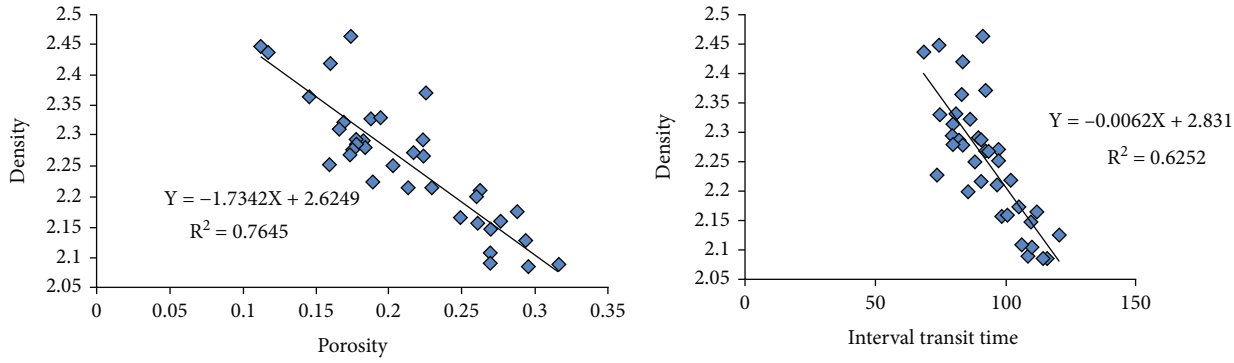

(a) (b)

Well	Formation	Core depth (m)	Thickness (m)	Core porosity		Porosity by formula	Error analysis	
				Sample quantity	Average		Absolute error	Relative error
A1	H1	2577.38–2583.04	5.66	11	9.8	9.5	−0.3	3.1
	H4	2928.31–2934.11	5.8	17	20.5	20.7	0.2	1
	H5	3020.01–3023.21	3.2	14	9.6	10	0.4	4.2
	H7	3289.31–3295.93	6.62	27	10.6	10.5	−0.1	0.9
	H8	3379.16–3384.281	5.12	23	14.3	14.1	−0.2	1.4
	H11	3550.29–3557.02	6.73	21	9.9	9.6	−0.3	3.0
B1	P1	3678.43–3687.06	8.63	47	8.5	8.3	−0.2	2.4
	P5	4062.95–4080.95	18	105	8.6	8.8	0.2	2.3
	P5	4080.95–4086.5	5.55	28	8.9	8.8	−0.1	1.1
C1	P5	4212.48–4220.58	8.1	9	8.1	8.4	0.3	3.7
	P8	4605.71–4620.67	14.96	13	7	7.2	0.2	2.9

(c)

Formula of porosity and interval transit time: Y = 0.0036X−0. 1188

(d)

Figure 2: Correlation and error comparison between porosity and interval transit time of Well B4: (a) the relationship of B4 Well between porosity and density; (b) the relationship of B4 Well between interval transit time and density; (c) correlation and error comparison of 3 random wells; (d) the equation of porosity and interval transit time obtained by combining two formulas (a) and (b).

analysis of organic geochemical indicators in this study include gray-black carbonaceous mudstone and dark mudstone, all of which were obtained from offshore drilling cores from the core library of Sinopec Shanghai Oil and Gas Branch. The pyrolysis experiments were completed in the State Key Laboratory of Continental Dynamics, Northwest University, and 27 samples were evaluated for organic matter abundance.

3.2. Seismic and Logging Data Interpretation. The 3D seismic and logging data in the study area are all from Sinopec Shanghai Oil and Gas Branch. The Landmark software is used for 3D seismic data interpretation, and the ResForm software is used for logging data interpretation. 3D seismic data are mainly used to determine the distribution characteristics and evolution of sedimentary facies, analyze the factors that control the development and distribution of coal-measure source rocks, and verify whether the reservoir contains hydrocarbons. The Landmark software can directly obtain the RMS amplitude, inversion distribution of unconventional reservoirs, and gas prediction based on seismic wave attenuation by calculating the 3D seismic volume. And well logs are used to differentiate between dark mudstone, carbonaceous mudstone, and coal seams, to calculate the percentage of each stratum and the porosity of the sandstone reservoir.

3.3. Sandstone Porosity Calculation. There are few porosity logging data in the study area, so the distribution of porosity cannot be calculated directly. However, the data of interval transit time and density are relatively complete, so the relationship between density and porosity and the relationship between interval transit time and density are used to jointly establish the relationship between porosity and interval transit time, so as to obtain porosity data by calculating the interval transit time data (Figures 2(a) and 2(b)). The correlation between the porosity and the interval transit time of Well B4 is the best, and it is selected as the background formula for porosity calculation. The relationship between the two is $Y = 0.0036X - 0.1188$ (Figure 2(d)). The porosity data obtained based on this relationship has a high coincidence rate with the measured porosity after correction (Figure 2(c)). Therefore, this relationship is used to calculate the porosity data of other wells, and then, the distribution of sand bodies with different porosity can be obtained by inversion.

3.4. Gas Detection Based on Seismic Wave Attenuation. Gas detection by attenuation method is based on the P-wave energy attenuation that occurs when seismic waves propagate in viscous formations [18, 19]. When the stratum contains hydrocarbons, especially gas, compared with nongas stratums, the low-frequency energy will be relatively increased, the high-frequency energy will be relatively

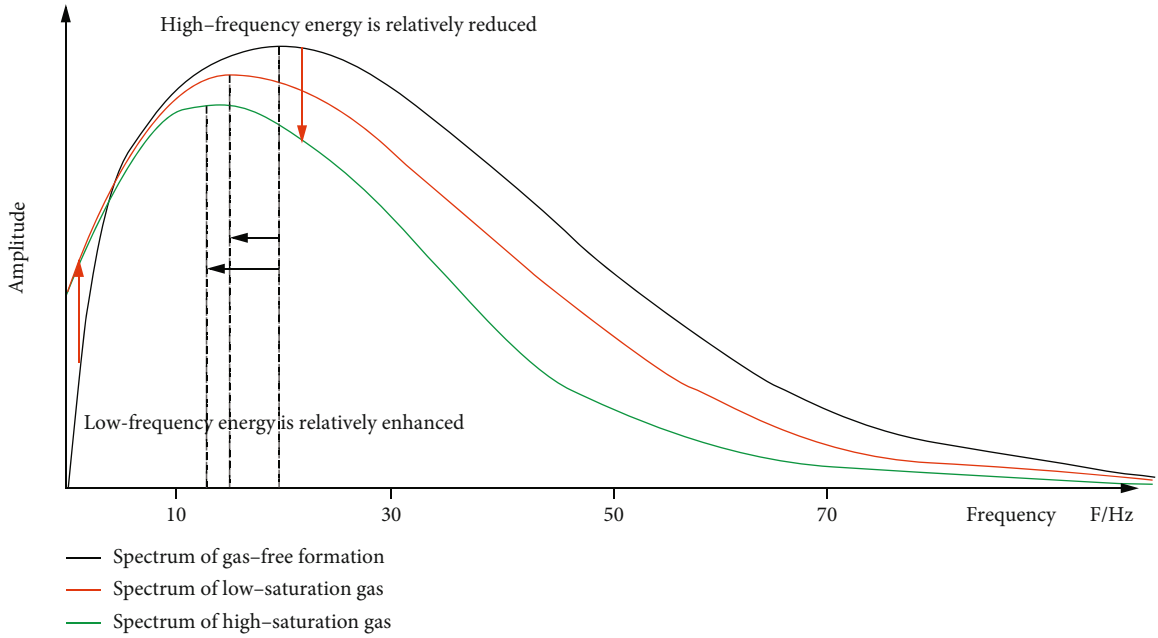

Figure 3: Comparison of frequency spectrum between gas-bearing stratum and nongas stratum.

reduced, and the peak frequency will decrease [19, 20] (Figure 3). The application of short-time discrete Fourier transform can effectively identify the existence of anomalous gas-bearing layers with attenuation. Perform discrete Fourier transform on the 3D seismic data volume with a large time window (50-100 ms); decompose the time domain seismic data into frequency energy volumes of 5 Hz, 10 Hz, 15 Hz, 20 Hz, 25 Hz, and 30 Hz; and calculate the energy difference between each frequency and its two sides, so as to identify the attenuation horizon and plane distribution within the 20-50 ms time window. Using this method, a gas layer with a cumulative thickness of 67.5 m was found in the delta front of the Zhuhai Formation in the Liwan 3-1 gas field [21] and an abnormal gas-bearing area of 20-62 km^2 in the seafloor fans of the Lower Zhuhai Formation in the Jieyang Sag [22].

4. Results

4.1. Abundance of Organic Matter in Source Rocks. Select source rock samples that basically cover the entire study area, carry out organic matter pyrolysis experiments, and analyze their geochemical characteristics. The pyrolysis results of 27 dark mudstone and carbonaceous mudstone samples (Table 1) show that the TOC distribution of carbonaceous mudstone ranges from 1.63 to 3.54, among which the carbonaceous mudstone reaches 3.54 in the T34 member of Well C1; the hydrocarbon generation potential is mainly distributed in the range of 0.15-2.35, up to 12.02; the kerogen types are mainly type II and type III, and type I is less. The organic carbon content of gray-black mudstone is distributed in the range of 0.4-1.66, which is lower than that of carbonaceous mudstone. Most of them belong to medium-grade source rocks, and the others belong to good source rocks; the distribution range of hydrocarbon generation potential of gray-black mudstone is 0.15-8.36, and most samples are greater than 1; carbonaceous mudstone has higher organic carbon content and hydrocarbon generation potential than dark mudstone. All samples are basically in the mature stage, and a few are in the immature stage. On the whole, the carbonaceous mudstone and dark mudstone in the study area have reached the mature stage and have begun to generate or have already expelled hydrocarbons.

4.2. Coal-Measure Source Rock Logging Distinction. Coal-measure source rocks and sandstones in the Pinghu Formation can be directly distinguished by logging curves, and the logging responses of the two are obviously different in low density, high interval transit time, low interval transit time, and low natural gamma. This study mainly distinguishes the coal-measure source rocks, which made up of the three types lithology including coal seam, carbonaceous mudstone, and dark mudstone. Due to the repeatability of the interval transit time and the natural gamma characteristics of the three, especially the dark mudstone and carbonaceous mudstone, all have high natural gamma logging responses, so it cannot be accurately distinguished only by observing the logging curves. In this regard, through the quantitative statistics of coal-measure source rock and sandstone logging data, it is mainly divided into five regions (Figure 4), and the lithology constraint formula of different regions can accurately and quantitatively calculate the content of various lithologies in the formation. The obtained lithologic quantitative constraints basically cover the entire study area, but there may also be some uncertainty due to incomplete data by the lack of logging curve in the T34 stratum.

4.3. The Relationship between Amplitude and Lithology. Idea of the research is to control a single variable, using logging constraints to correspond to different lithology performances,

Table 1: Pyrolysis results of carbonaceous mudstone and dark mudstone.

Sample number	Well number	Depth (m)	Formation	Lithology	TOC (%)	Tmax (°C)	S1 + S2 (mg/g)	Parent material	Evolutionary phase
1	A1	3546	T32	Mudstone	1.19	445	2.99	IIA	Mature
2	A1	3568	T32	Mudstone	0.8	445	0.75	IIB	Mature
3	A1	3569	T32	Mudstone	0.83	446	0.67	III	Mature
4	B1	3494	T31	Mudstone	0.68	437	0.29	III	Mature
5	B2	3391	T31	Mudstone	0.6	392	0.23		
6	B2	3807	T34	Mudstone	1.41	438	8.36	I	Mature
7	B2	3808	T34	Mudstone	1.66	444	2.74	IIB	Mature
8	B2	4090	T34	Mudstone	0.98	453	1.23	IIA	Mature
9	B2	4061	T34	Mudstone	0.64	457	0.44	IIB	High mature
10	B3	3273	T31	Mudstone	1.38	433	1.58	III	Mature
11	B3	3398	T34	Mudstone	0.6	405	0.37	III	Immature
12	B3	3629	T34	Mudstone	0.4	422	0.17	III	Immature
13	B3	3627	T34	Mudstone	0.5	410	0.2	III	Immature
14	B4	3652	T32	Mudstone	0.77	437	0.66	III	Mature
15	B4	3961	T34	Mudstone	0.72	446	0.74	IIB	Mature
16	C1	3156	T32	Mudstone	0.53	463	0.18	III	High mature
17	C1	3321	T32	Carbonaceous mudstone	1.63	444	2.35	IIB	Mature
18	C1	3322	T32	Mudstone	0.47	432	0.15	III	Mature
19	C1	3635	T34	Mudstone	3.54	446	12.02	IIA	Mature
20	D1	4513	T34	Carbonaceous mudstone	2.06	468	2.77		
21	E1	3811	T31	Mudstone	0.53	451	0.43	IIB	Mature

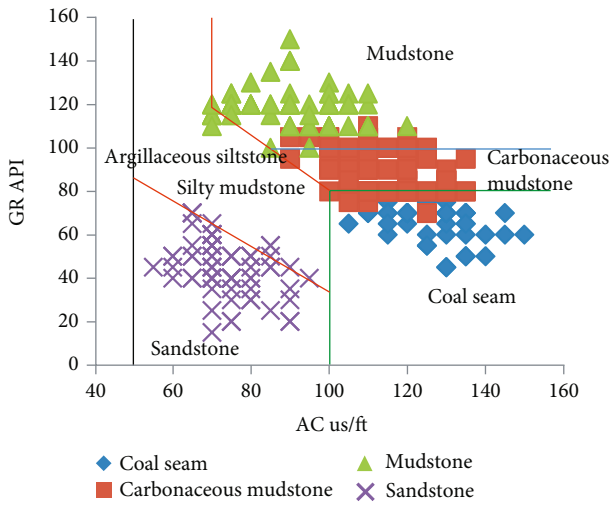

Figure 4: Logging differentiation of lithology in reservoir sandstone, source rock, and transition rock.

changing logging conditions to achieve changes in corresponding lithology, and then observe the changes in amplitude. High interval transit time and low natural gamma logging response correspond to high organic-rich shale; low interval transit time and low natural gamma logging response correspond to reservoir sandstone. Changing the interval transit time and natural gamma value of shale and sandstone is to observe the law of amplitude change.

There are two sections of 8 m-thick sandstone and 6 m-thick shale at the depth of 3000 ms (T31-T32) in Well A1 (Figure 5(a)), corresponding to medium and strong amplitudes, respectively. When the interval transit time and natural gamma value of the 8 m-thick sandstone are increased, it becomes mudstone, and the amplitude changes accordingly, and the medium amplitude weakens (Figure 5(b)); after reducing the interval transit time and natural gamma value of 6 m thick shale, the amplitude also weakens, and the strong amplitude weakens (Figure 5(c)). This law is universal in the study area. Therefore, the relationship between amplitude and lithology can be summarized as follows: the amplitude is negatively correlated with silty mudstone or argillaceous siltstone and positively correlated with sandstone and shale with high organic content.

5. Discussion

5.1. Evolution and Main Controlling Factors of Sedimentary Facies. At present, the sedimentary research on the Pinghu Formation believes that the transition and semiclosed bays are the main depositional environments, the northern sedimentary facies are dominated by the tidal-delta system, and the central and southern parts develop semiclosed bays. Compared with the delta facies, the tidal flat-lagoon

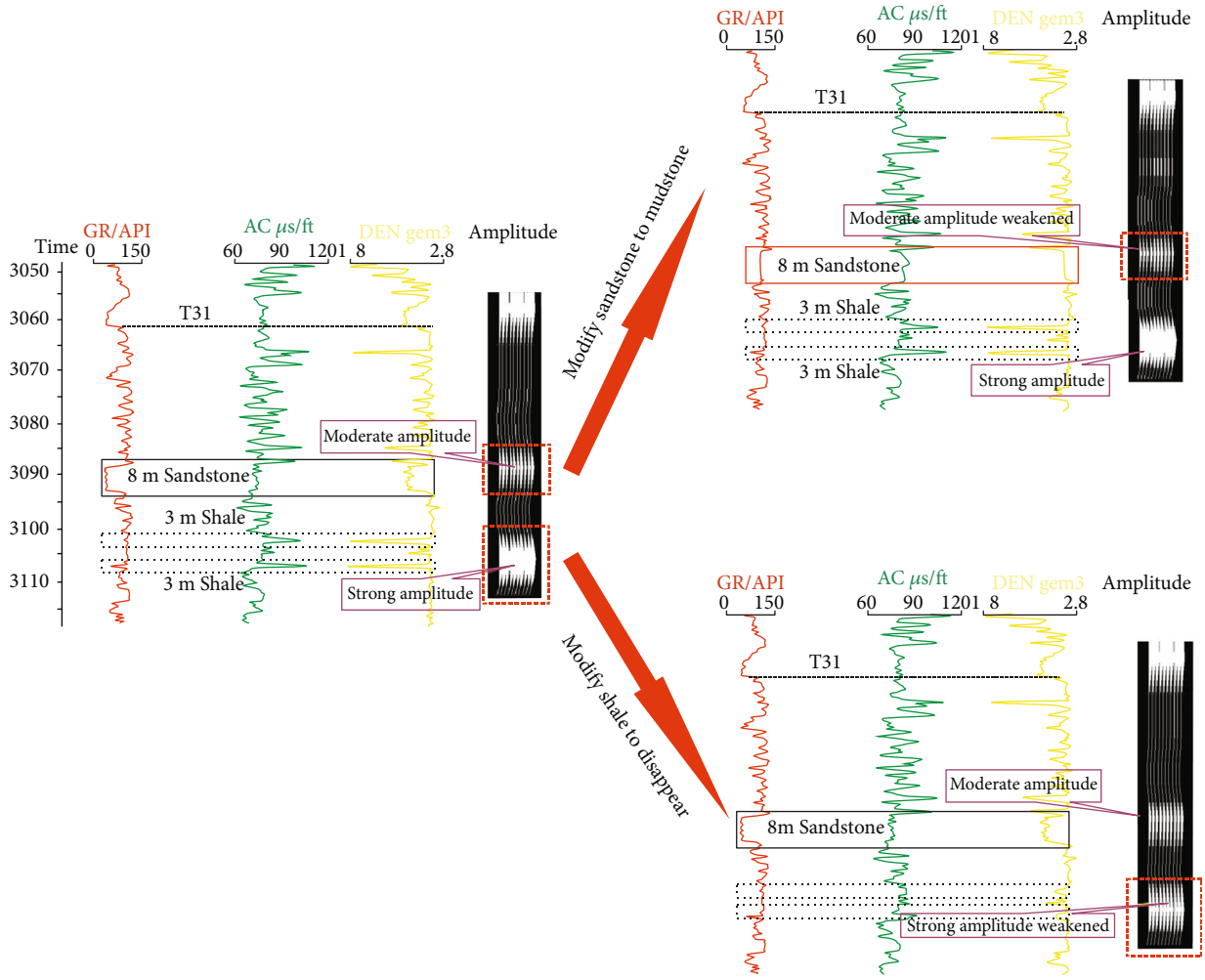

Figure 5: Amplitude corresponding to lithology change: (a) original lithology corresponds to amplitude; (b) lithology, which modifies sandstone to mudstone, corresponds to the weaken amplitude; (c) lithology, which modifies shale disappeared, corresponds to the weaken amplitude.

sedimentary system has higher potential for coal development [23]. However, the main controlling factors of delta facies have always been controversial, and different scholars have different views. Some scholars believe that the sedimentary facies of the Pinghu Formation belong to the tidal-controlled delta facies, and it develop tidal delta subfacies, delta-front subfacies, and predelta subfacies [24]; some scholars believe that the delta facies is dominated by tides and waves, and the deposition is corresponding to tide-controlled deltas and wave-controlled deltas [25]; and some scholars believe that tide is not the main controlling factor, but delta deposition dominated by river and wave [26]. In this regard, the author judges its controlling factors based on the plane shape and scale of the strong earthquake amplitude and believes that the delta facies developed in the Pinghu Formation in the study area are jointly controlled by braided channels, waves, and tides and are affected by transgression and regression. And it developed braided river delta facies, wave delta facies, and tidal flat facies.

The sand body shape and scale represented by strong amplitudes reflect depositional control factors. Wave-controlled sand bodies are leaf-shaped, river-controlled sand bodies are bird's foot-shaped, and tide-controlled sand bodies are bay-shaped [20]. The delta deposition controlled by different factors directly determines the physical properties of the reservoir and affects the enrichment of oil and gas [27, 28]. Scruton classifies deltas into constructive and destructive based on deposition rates [29]. Fisher and Mcgowen believe that constructive deltas are leaf-shaped and destructive deltas are beak-shaped [30]. At the same time, the research on the provenance of the Xihu Sag believes that there are three main provenance areas in the Xihu Sag, the northern part is from the Hupi Reef Uplift, and the southeast is from the Sea Reef Uplift and the Diaoyu Island uplift [31]. The provenance of the Pinghu Formation in the study area mostly comes from the western uplift area, and the Pingbei area is greatly affected by the provenance in the northwest direction, so the sand bodies are mostly accumulated and developed in the Pingbei-Pingzhong area.

The strong red amplitude reflecting the sand body shows two forms in the study area: curved narrow-band shape and flower shape. The sedimentary microfacies determines the

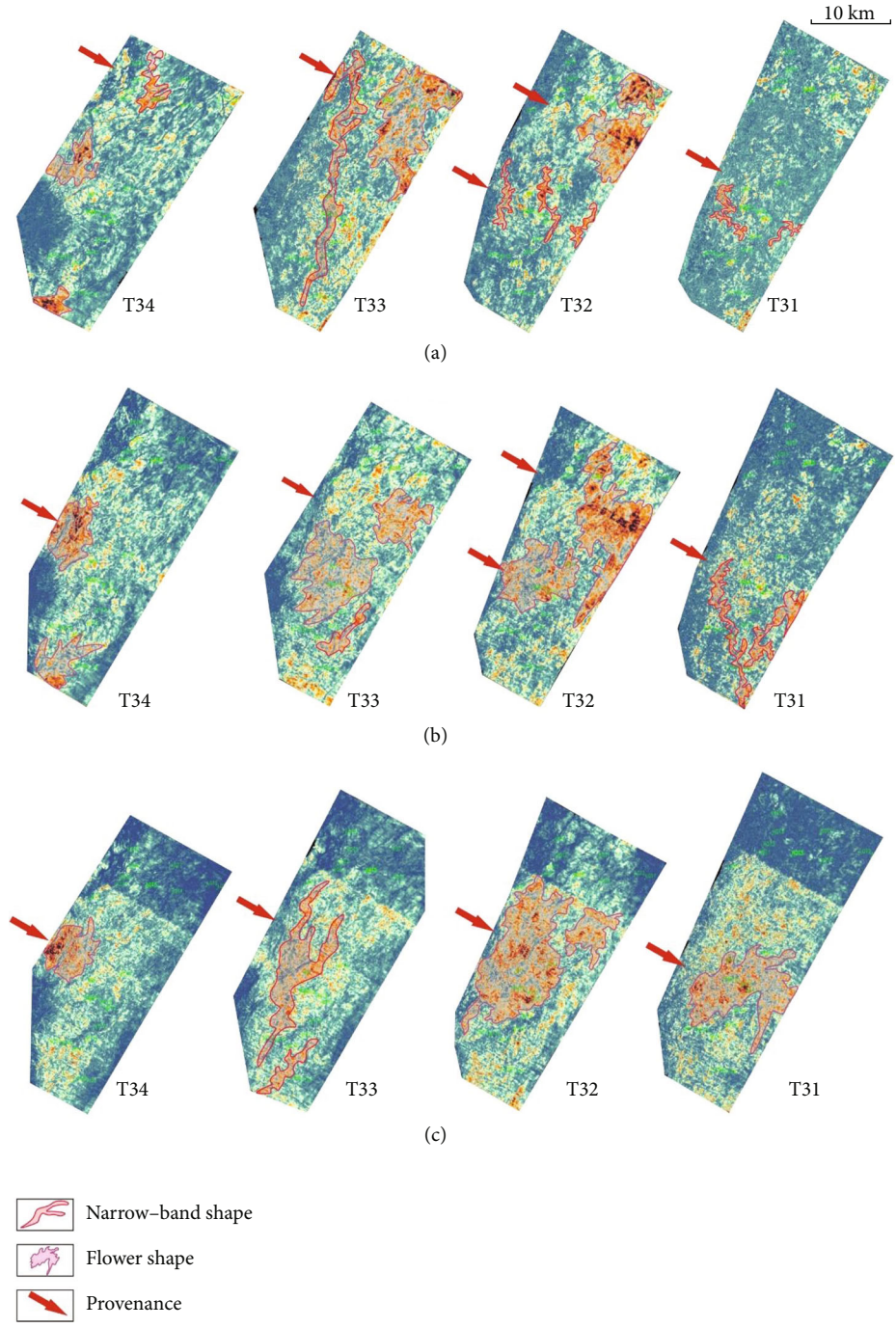

Figure 6: Shape distribution of strong earthquake amplitudes corresponding to sand bodies with different thicknesses.

plane distribution of the sand body. The narrow-band shape reflects the underwater distributary channel microfacies, and the flower shape reflects the wave-controlled distributary river mouth-bar microfacies. And the sand body thicknesses represented by different frequencies are also different (Figure 6). According to the change of sand body shape, it can be seen that the river-controlled delta distributary channel microfacies, the wave-controlled delta distributary channel microfacies, and the tide-controlled delta facies developed alternately from T34 to T31, and the sand bodies are dominated by each other. According to the moving trend of sand bodies along the coastline, it is believed that transgression and regression occurred alternately during the depositional period of the Pinghu Formation. Regression causes the coastline to move away from the land, and the decline of sea level causes the development of wave-controlled and tide-controlled deltas to be restricted. The sedimentary facies are dominated by river-controlled delta facies, which are favorable for the growth and development of strip-shaped sand bodies and higher plants in swamp

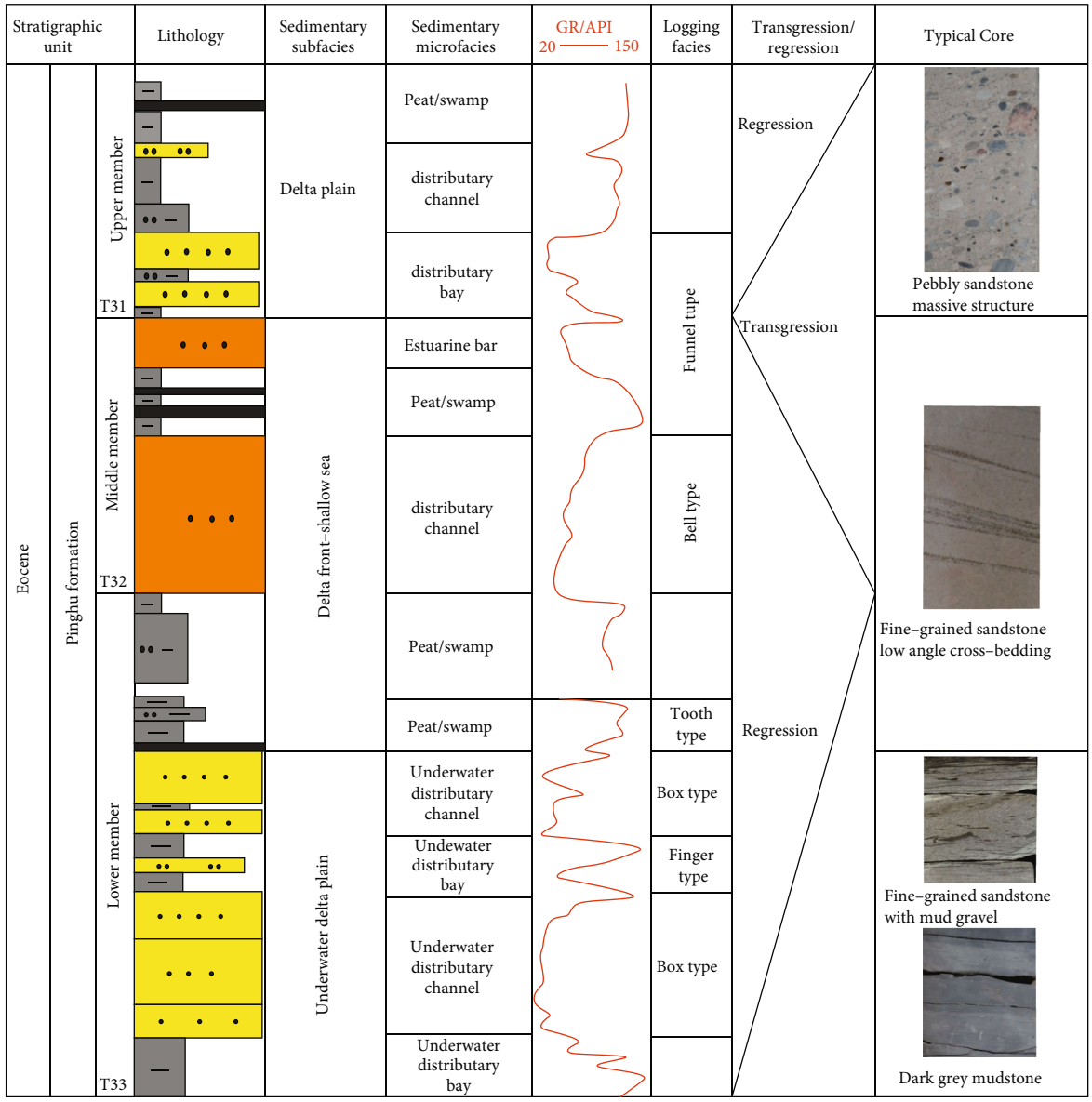

Figure 7: Sedimentary characteristics and evolution of the Pinghu Formation.

environments, as well as the development of reservoirs and coal seams. The transgression is just the opposite, the coastline advances to the continental slope belt, and the sedimentary development of sand body is affected by the wave-controlled and tide-controlled delta facies. The cause of deposition of large sets of thick sand bodies also changed from delta distributary channel microfacies to wave-controlled river mouth-bar microfacies. The deeper underwater environment also provides a more stable reducing environment, which is conducive to the development of carbonaceous mudstone and dark mudstone. The sedimentary evolution model of the Pinghu Formation in the study area can be summarized as follows: starting from T34, affected by two stages of regression and one stage of transgression, the sedimentary facies has undergone a transformation process, from transitional facies (delta front-pre-delta-shallow sea), underwater delta plain subfacies to distributary channel subfacies, delta front subfacies to delta plain subfacies (Figure 7).

5.2. Controlling Factors of the Coal-Measure Source Rock's Distribution

5.2.1. Control of Sedimentary Facies. The development of source rocks is affected by specific sedimentary facies. Studies have shown that the high organic matter of surface water and the anoxic preservation conditions of bottom water are very important when source rocks are formed [32]. The high productivity of organic matter is conducive to the formation of coal-measure source rocks, and the stable water in anoxic environment is conducive to the preservation of organic carbon. Marine source rocks of China are

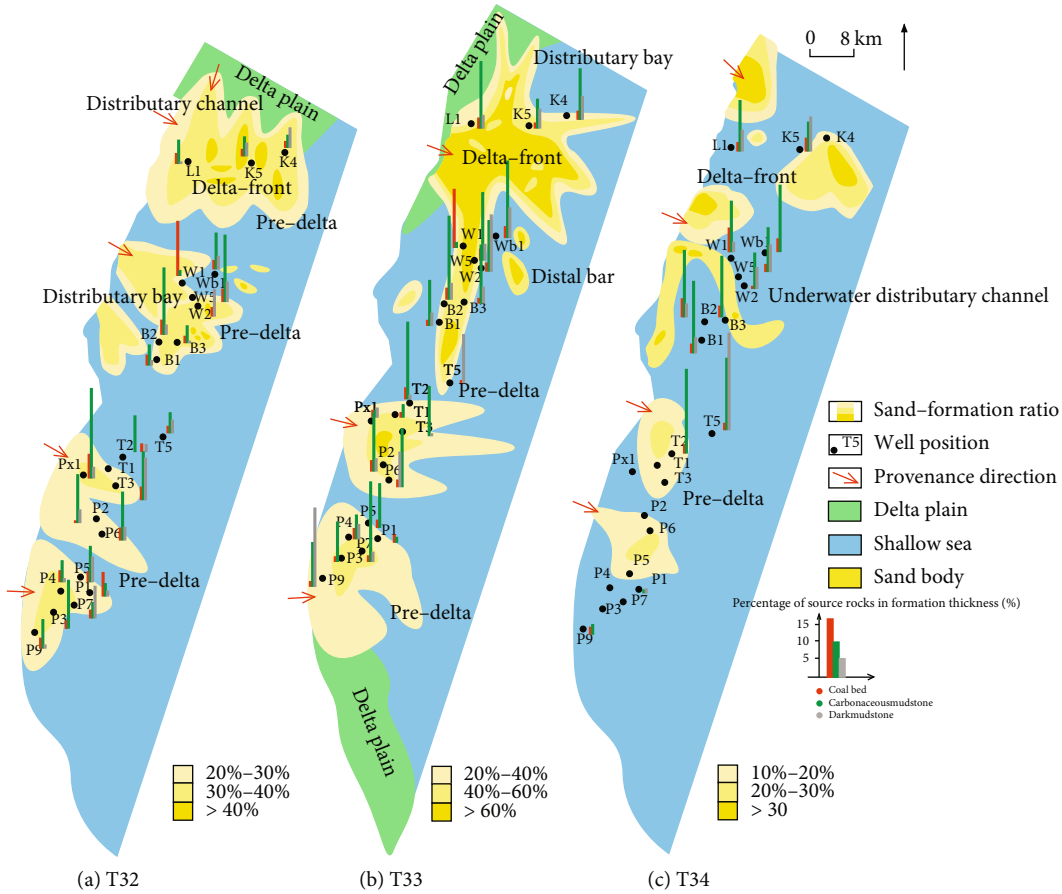

Figure 8: Schematic diagram of the relationship between the distribution of source rocks and the development of sedimentary facies: (a) development and distribution of source rocks in delta-front-shallow sea sedimentary facies during the period of T32; (b) development and distribution of source rocks in delta plain sedimentary facies during the period of T33; (c) development and distribution of source rocks in delta-front-shallow sea sedimentary facies during the period of T34.

mainly developed in terrigenous bay facies, gentle slope facies, lacustrine swamp facies and predelta, etc. [33]. The coal-measure source rocks in the study area satisfy the development conditions of gentle slope facies and delta facies at the same time. The gentle slope facies are related to the structure, and this chapter discusses the influence of the wave-controlled delta facies in NE banded shape on the formation and preservation of source rocks under transgressive and regressive environments.

The source rocks in the study area are affected by the delta plain subfacies, the delta front subfacies, and the predelta subfacies. The thicknesses of source rocks and sandstones are counted, and it is considered that transgression and regression are the dominant factors affecting their thickness variations (Figure 8). The predelta subfacies was dominated during the T34 period, but the source rocks and sandstones of the plain subfacies and delta front subfacies were thicker. The T33 period is dominated by the delta plain subfacies, and the thickness of development from large to small is the plain subfacies, the front subfacies, and the predelta subfacies. The T32 period is dominated by the delta front subfacies, which is more developed than the plain and predelta subfacies. In general, the sand-mudstone deposition in the study area is controlled by the delta plain subfacies and the delta front subfacies, and the predelta subfacies is relatively weak. Coal-measure source rocks are controlled by interdistributary bay and swamp deposits in the plain subfacies, and the sequence from top to bottom is predelta mudstone and organic swamp. The delta front subfacies and the predelta subfacies are mostly sandstone deposits, and a small amount of organic mudstone may be deposited by the water impact from upriver plain to the offshore area.

Sandstone deposition depends on the microfacies such as distributary channel and mouth bar controlled by the plain subfacies and front subfacies during the period of T32 and T33. During the deposition period of T34, the predelta subfacies was the main sedimentary facies, and the accumulation of sand body should mainly depend on the estuarine bars. However, the statistical results show that the control ability of the plain subfacies and the front subfacies to sand bodies is much greater than that of the predelta subfacies (Figure 9). In this regard, it is reasonable to think that the waves were the main controlling factor of the delta deposition at that time, and the impact intensity on the land was very strong, which belonged to the destructive delta deposition under the wave control. The strong impact on the mouth bar sand bodies resulted in the loss of sand bodies

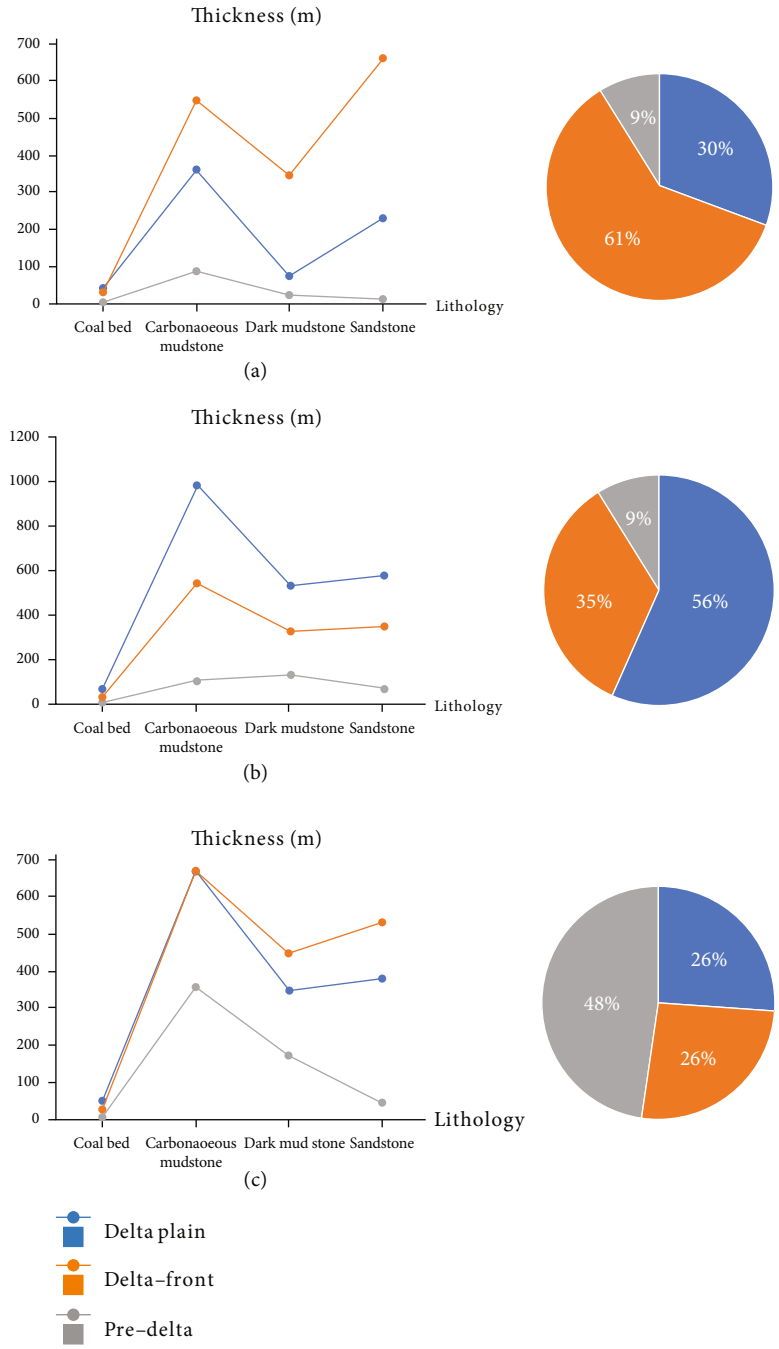

Figure 9: The relationship between content of source rock, sandstone, and sedimentary subfacies: (a) depositional thickness of various lithologies and distribution of study wells in various sedimentary subfacies during the T32 period; (b) depositional thickness of various lithologies and distribution of study wells in various sedimentary subfacies during the T33 period; (c) depositional thickness of various lithologies and distribution of study wells in various sedimentary subfacies during the T34 period.

and the ineffective accumulation of sand bodies, so the development of sand bodies in the predelta subfacies was low, and it also confirmed that there was indeed a transgression during the period of T34. Moreover, the source rocks in the P Well area were hardly developed during the period of T34, indicating that they were also inhibited by ocean waves. The high-reducing environment of short term caused by it inhibits the formation of organic carbon, and the preservation conditions are also damaged by the impact of waves. Therefore, the more stable plain subfacies and front subfacies are more conducive to the development and preservation of coal-measure source rocks and sandstone reservoirs.

5.2.2. Control of Terrain. Some studies believe that the development of source rocks on the slope of the Pinghu Tectonic Belt is different from that near the inner side of the sag. The source rock in the slope belt is thicker and has great potential of hydrocarbon generation; there are also studies that

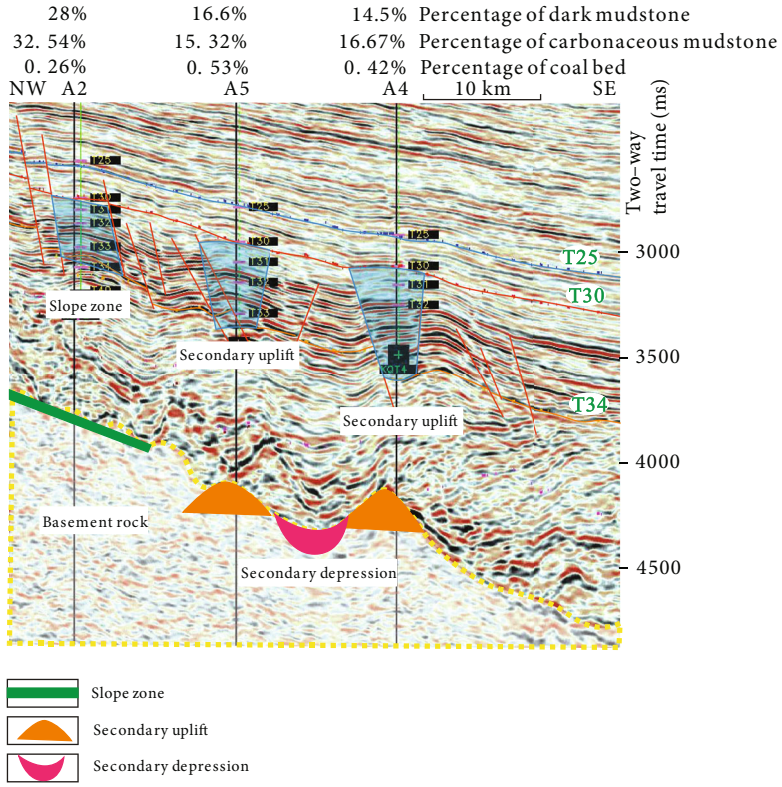

Figure 10: Relationship between terrain and the development of coal-measure source rock in Well Block A.

suggest that the slope angle of the Pinghu Tectonic Belt is approximately 0.23-3.2. The coal seam and carbonaceous mudstone have higher content in the calm-water area with larger slope angle and lower water level. The dark mudstone has higher content in the deep-water area with smaller slope angle [13]. Therefore, whether the slope is steep or gentle, and the structural feature will have a greater impact on the development and distribution of source rocks.

The structures of secondary uplift and depression in the study area are influenced by the tensile-compressive stress of the plate and are formed based on the basement. Secondary structures directly affect the growth and development of coal-measure source rocks. The oxidation and reduction environment on which the source rock development depends is controlled by the water level, and the structural height directly determines the developmental environment of source rock. The oxidation environment with shallow water formed by the secondary uplift is favorable for the development of coal seams, and the anaerobic reduction environment formed by the secondary depression is favorable for the development of dark mudstone. The source rock content in Well Block A reflects this law (Figure 10). Wells A5 (0.53%) and A4 (0.42%) are located at the local high points of the secondary uplifts, with relatively flat terrain and relatively lower water level. The oxygen-rich environment is conducive to growth of higher plant. Compared with the slope where Well A2 (0.26%) is located, the growth and preservation of coal seam are better. The oxygen-rich environment is not conducive to the development of dark mudstone, and the percentage of dark mudstone is lower than that of the slope. The slope zone is in a transitional environment of high oxygen and low oxygen, and the organic matter content changes from high to low. The content of carbonaceous mudstone is as high as 32.54%, which is better than that of secondary uplift.

5.2.3. Control of Hanging Wall and Footwall Faults. During the development period of coal measure source rocks in the Pinghu Formation, the Xihu Sag was in the transition period of fault-depression. Fault-terrace assemblages are developed, which have a controlling effect on stratigraphic deposition and have a significant impact on the development of source rocks [34]. The essential effect of the upfaulted and down-faulted control on the source rocks is whether the oxidative and reducing environment caused by the rise or fall of the water level is conducive to the growth of organic plant. The hanging wall causes the stratum to rise locally. Even if the sea level rises due to transgression, the vegetation will not be completely submerged. The hanging wall provides a stable oxidation environment for coal seams and carbonaceous mudstone; in contrast to the footwall, the stratum descends locally, and the reduction environment of stable deep-water is conducive to the formation and preservation of dark mudstones. During the depositional period of the Pinghu Formation in the study area, the faults were highly developed and distributed in a north-south banded shape on the plane. The strata controlled by them were located in different depositional environments, resulting in different degrees of development of source rocks. Wells K3 (0.15%) and K4 (0.32%) were deposited on the footwall of the fault,

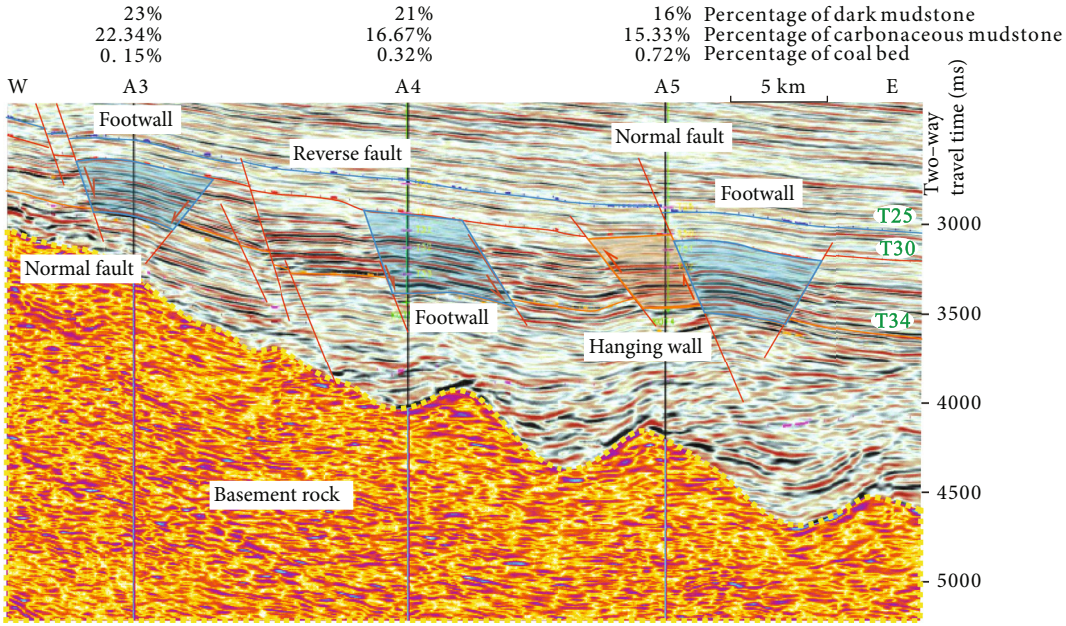

Figure 11: Control of faults on coal-measure source rock.

respectively (Figure 11). The stratum descends to form a larger sedimentary space, and the water depth increases to provide an anaerobic environment, which is conducive to the development and preservation of dark mudstone and carbonaceous mudstone; the well K5 (0.72%) is located on the hanging wall of the fault. The rise of the stratum causes sea level to decrease relative to the stratum, providing an oxygen-rich oxidation environment, which is conducive to the development of coal seams, and the storage conditions of dark mudstone and carbonaceous mudstone are poor.

5.3. Distribution of "Sweet Spots" for Coalbed Methane and Shale Gas and Their Controlling Factors. The formation and preservation of coalbed methane is related to the evolution of the basin, stress field, multiple structures, and water conditions [35, 36], and its enrichment models can be summarized as the model of hydrodynamic-controlled accumulation, the model of syncline-controlled reservoir, the model of accumulation for relatively high structure, and the model of enrichment for slope zone. The structural form of the study area plays a key role in the preservation of coalbed methane. Generally speaking, the overlying stratum on the syncline is in a state of extruding stress on both sides of the fold, and faults and fissures are not developed, which is conducive to the preservation of coalbed methane; the anticlinal strata are subject to tensile stress, and the tension is prone to fracture and cracks, which is not conducive to the preservation of coalbed methane. The Pinghu Tectonic Belt is located in the footwall of the faulted basin, and the sedimentary strata are mainly developed in the sag, and the extruding stress is conducive to the preservation of coalbed methane. The development and preservation of shale gas are mainly affected by the depositional environment, and its types of reservoirs are generally divided into organic pores of marine shale, diagenetic microfractures of transitional shale, and bedding fractures of continental shale. The sedimentary environment of the study area is dominated by marine-continent transitional facies and marine facies, and the shale of marine-continent transitional facies and marine facies is widely developed. Both gas-generating conditions and storage conditions of gas greatly endow possibilities for shale gas accumulation in the study area [37].

The thickness distribution of coal-measure source rock caculated quantitatively according to the logging constraints in Figure 12. There are roughly 3-5 hydrocarbon-generating depressions in the coal-measure source rocks during the period of T31 and T32 in the study area, which are distributed like a pearl in NE direction. Compared with coal seam and dark mudstone, carbonaceous mudstone has the thickest development. The maximum thickness can be up to 80 m, the thickness of dark mudstone is up to 40 m, and the coal seam is relatively thin. Coal seams, carbonaceous mudstone, and dark mudstone are all developed and distributed in these hydrocarbon-generating depressions. Affected by the water depth caused by the depositional environment, the distribution range of coal seams is small, and the distribution range of carbonaceous mudstone and dark mudstone is relatively large. Overall, distribution of "sweet spot" in vertical shows that the degree of development and preservation of coalbed methane and shale gas in the T32 formation is better than that in the T31 formation. It is related to the change of sedimentary environment caused by transgression and regression during the depositional period, and the decrease of reservoir porosity and the increased degree of thermal evolution caused by burial depth. The decrease of reservoir porosity directly leads to the decrease of reservoir permeability. According to the existing exploration and development experience of coalbed methane, it is believed that low permeability is the key condition for coalbed methane accumulation. The permeability value of sandstone

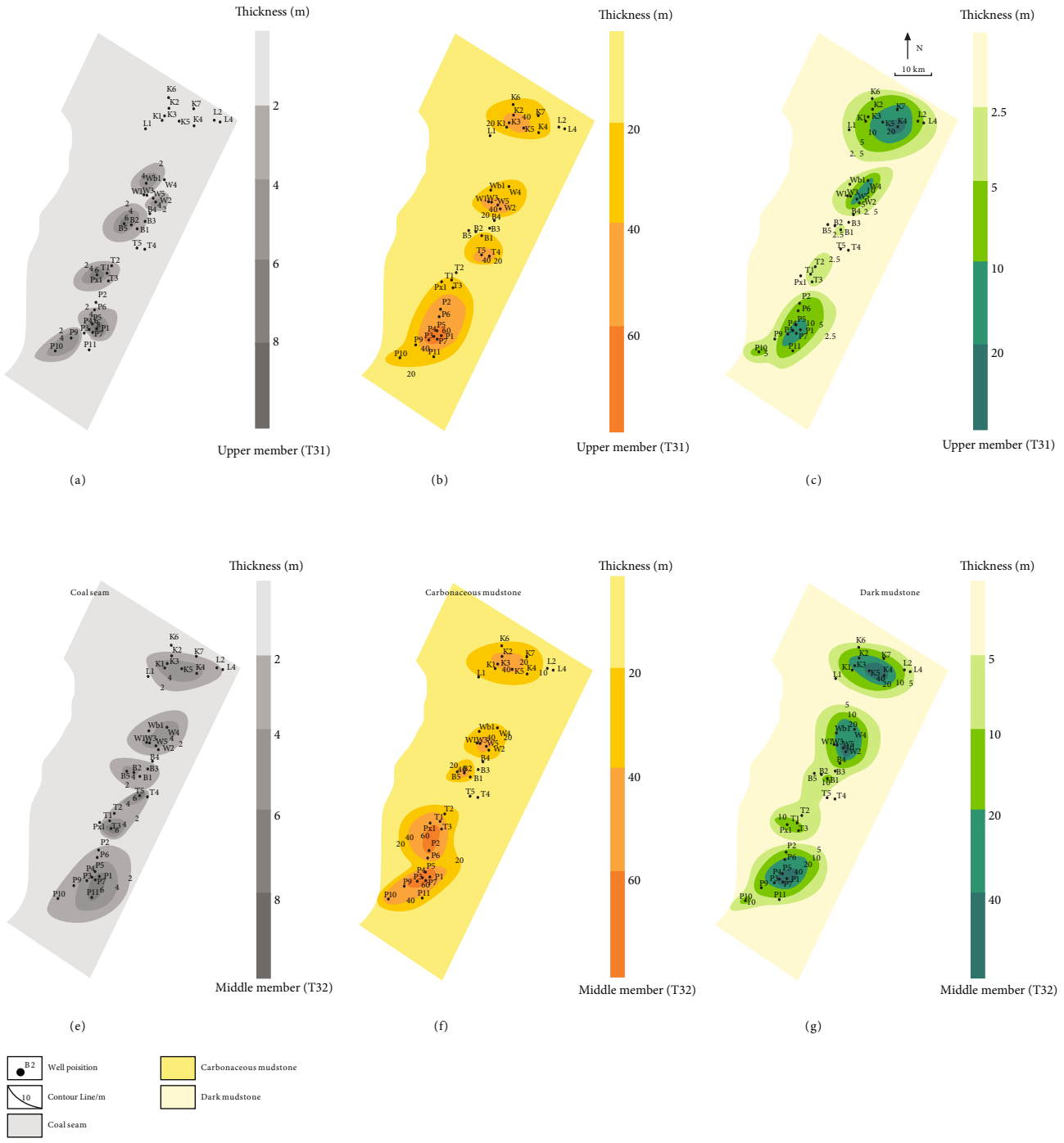

Figure 12: Development and distribution of coal-measure source rocks in the upper member (T31) and middle member (T32).

reservoir in the Pinghu Formation is generally low, which can satisfy the accumulation of coalbed methane. The degree of thermal evolution is positively correlated with the burial depth. The vitrinite reflectance (Ro), which reflects the degree of thermal evolution, increases with the increase of burial depth of the stratum. [38]. The analysis shows that the paleotemperature of T32 stratum in the Pinghu Tectonic Belt is 163°C, and the vitrinite reflectance reaches 1.26%; the paleotemperature of the overlying T31 stratum is 134°C, and the vitrinite reflectance can reach 1.14%. In contrast, the vitrinite reflectance of the gas generation threshold in the Xihu Sag is 0.80% [39]. It shows that the coal seam of T32 stratum is more likely to reach the gas generation threshold first, and the thermal evolution degree of the T32 stratum with a greater burial depth is higher than that of the T31 stratum, and it is more likely to generate coalbed methane. The "sweet spots" of the reservoir are better in the south than in the north on the plane. The reason for this distribution may lie in the period of

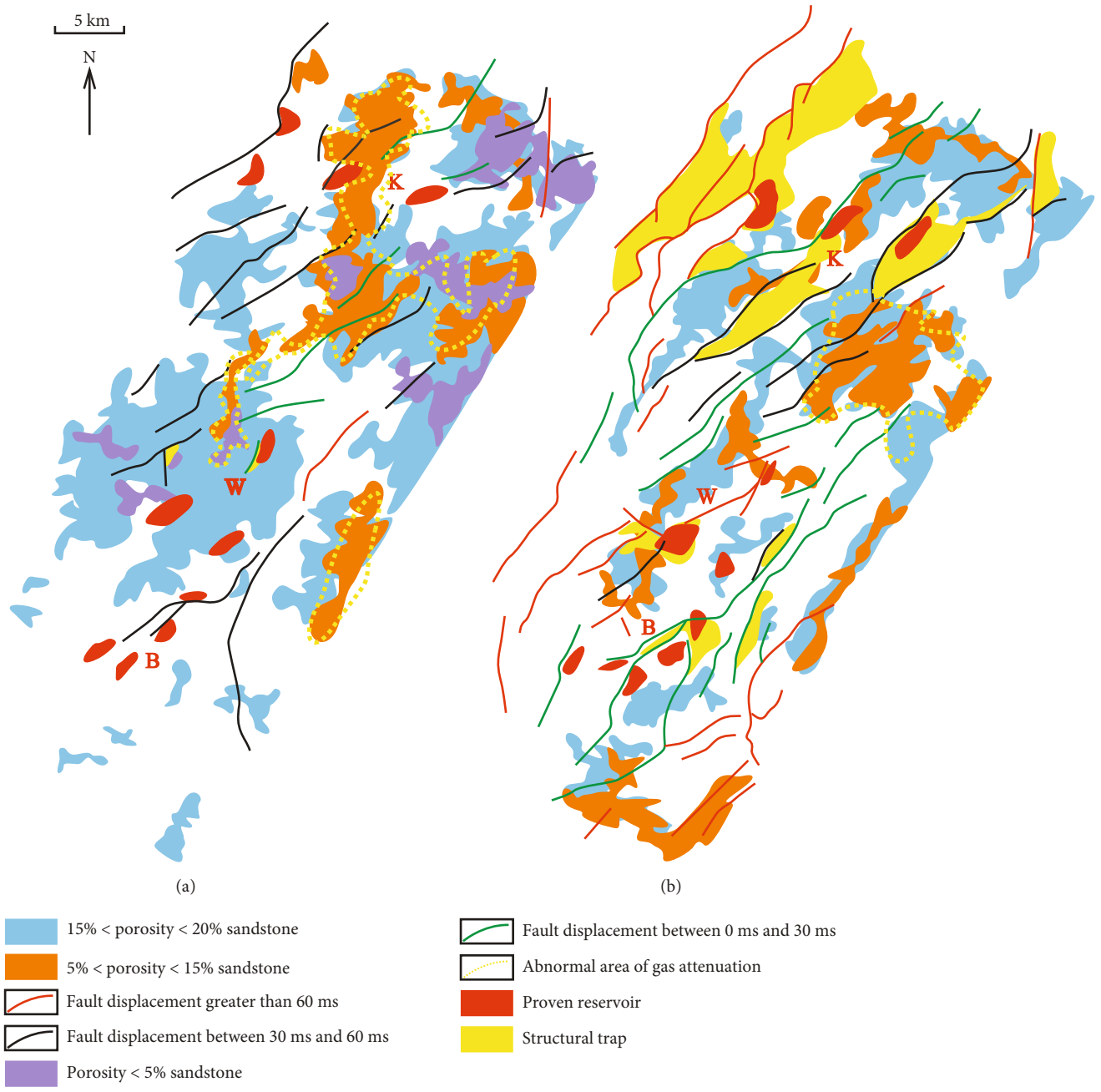

Figure 13: The relationship between the "sweet spots" of tight oil and gas reservoirs and the distribution of different faults: (a) tight reservoir distribution and prediction of gas-bearing traps in T31 period; (b) tight reservoir distribution and prediction of gas-bearing traps in T32 period.

T31, the provenance area is mainly in the south, and the lack of sediment sources in the north leads to the lack of shale development. In addition, from the North Pinghu area to South Pinghu area, the slope of the marginal faulted basin from gentle to steep (Figures 1(c)–1(f)). The large height difference produced by the steep slope and the fracture works together, which is conducive to the formation of the depression. The extruding stress necessary to form the depression can create a closed space, which is not conducive to the escape of gas.

5.4. Accumulation Analysis of Tight Sandstone Oil and Gas. The Xihu Sag is affected by diagenesis, and the target layer is buried deeper than 3000 m, which is generally a tight reservoir. The Pinghu Formation is the focus of research on tight reservoirs in the Xihu Sag. According to the calculated data of sandstone porosity and its seismic inversion, the porosity of sand bodies in the Pinghu Formation can be divided into three grades (Figure 13): 15%-20%, 5%-15%, and <5%. The formation of sand bodies with porosity < 5% is affected by wave-controlled deltas; the formation of sand

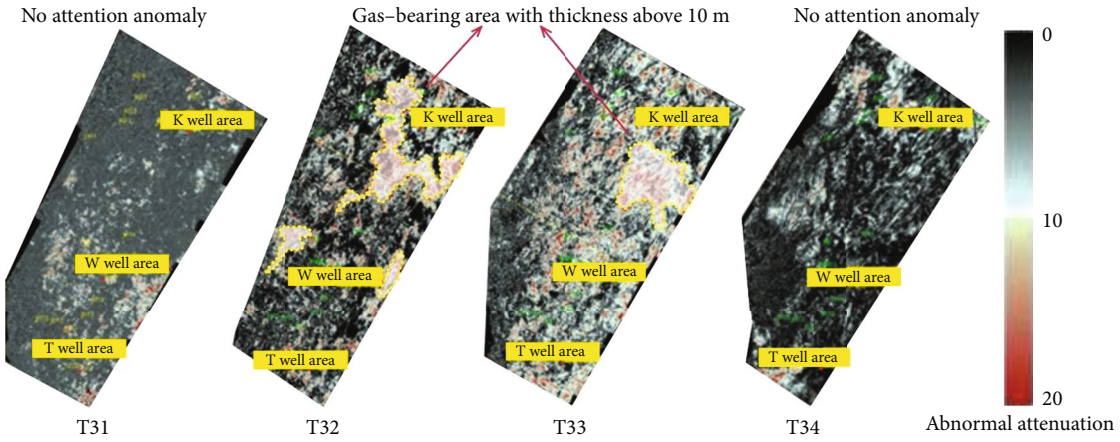

Figure 14: Prediction of gas-bearing traps by seismic wave attenuation method in Pinghu Formation.

bodies with a porosity of 5%-15% is affected by river-controlled and wave-controlled deltas; sand bodies with porosity > 15% are mainly distributed on the west side of the slope belt near the terrestrial sources, close to the delta plain. The formation of sand bodies is controlled by distributary channel microfacies of the delta and may also include some tidal pores and wave-controlled point sand bars. Among the proven oil and gas reservoirs, the vast majority of the reservoirs are tight sand bodies with a porosity of 5%-10%. And most of the sand bodies are narrow-banded, indicating that the distributary channel facies of the delta easily form tight sand body reservoirs.

Some research has been carried out on the reasons for the densification of the reservoirs and the accumulation conditions of the tight reservoirs [40, 41]. It is believed that the tight reservoirs in the Pinghu Formation are mainly composed of arkose and quartzose arkose, cemented calcite, and dolomite. The porosity of the middle and lower members of the Pinghu Formation is concentrated between 2% and 20%, with an average porosity of 10%. The formation of tight sandstone reservoirs is closely related to sedimentary facies. The study of facies control shows that sedimentary facies is dominated by river-controlled and wave-controlled underwater distributary channels of the delta, with flower-shaped delta front sand bodies and mouth bar sand bodies developed in the Pingbei-Pingzhong area. The sedimentary system of delta sand body and barrier coast-tidal developed by tide control are second. Because the wave-controlled delta and tidal sediments are mainly composed of medium sandstones and fine sandstones, the overall grain size is relatively coarse, the maturity is high, and the grain sorting is good. Therefore, the single-layer thickness of the tight sandstone reservoir is between 5 and 30 m, the sand-formation ratio is between 20% and 40%, and the porosity is between 5% and 15%, which provides good reservoir conditions for tight oil and gas accumulation. The porosity of tight reservoirs in Xihu Sag is greatly affected by later diagenesis, including compaction, cementation, and dissolution [42]. The compaction produced by the deep sandstone of the Pinghu Formation is affected by the large burial depth and the greater effect of temperature and pressure, and the intensity of physical and chemical compaction is stronger than that of the overlying sandstone. Cementation plays an important role in the quality improvement of deep reservoir sandstone. There are two types of calcite cementation: early stage and late stage. In the early stage, most of them are basement-type contiguous cementation, and in the late stage, veins of coarse crystal are mainly filled in the fractures. It is analyzed that it is related to the Longjing Movement [43]. Early calcite cementation is most developed at the mud-sand interface [44], but it is affected by the superposition of reservoir sand bodies and channel erosion. Calcite cementation is only distributed at the mud-sand interface and has a limited range, so it has little effect on the modification of reservoir porosity. The difference in dissolution in the study area depends on the intrusion of corrosive fluid and the changes in the opening and closing of the diagenetic system and is related to whether the acid-bearing body of organic matter can enter the reservoir smoothly [45]. The dissolution of the Pinghu Formation reservoirs is related to the Huagang Movement and the Longjing Movement [46]. Under the action of the Huagang Movement, when the oil and gas began to charge into the reservoir in the early stage, the organic acid fluid began to enter the reservoir. During the Longjing Movement, the charging movement was still in progress, which was accompanied by a large-scale reformation of reservoir porosity.

Using the gas detection method by seismic attenuation, it is believed that there exist red positive attenuation anomalies that may represent hydrocarbons in the strata of T32 and T33 (Figure 14). The red attenuation area is a regional hydrocarbon-bearing reflection, which is the performance of different calculation between the frequency division of the hydrocarbon-bearing layer and that of the upper and lower strata. In order to verify whether the red attenuation area reflects the real gas content, the red attenuation area of the T33 stratum corresponds to the depth-domain frequency division. Red-yellow area of the cross section is obviously different from the blue-green area, showing abnormal energy of hydrocarbon-containing. It can be seen that the

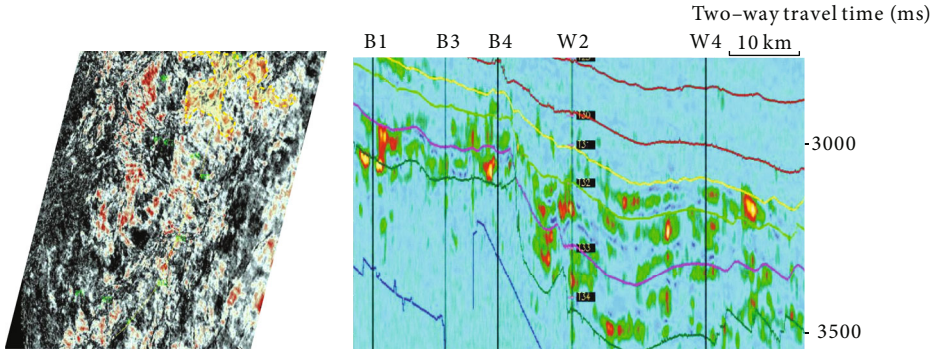

FIGURE 15: Coincidence verification between prediction of gas-bearing traps and high-frequency gas layer in T32 period: (a) distribution of gas trap in plane; (b) longitudinal distribution of high-frequency gas-bearing formations.

anomaly area of red attenuation is indeed consistent with the hydrocarbon-bearing anomaly area (Figure 10).

In connection with the distribution of tight sand bodies (Figure 15), gas-bearing anomalies are mainly concentrated in the areas with reservoir porosity of 5%-15%, including a few sandstones less than 5%. However, sandstone reservoirs with porosity > 15% contain less gas, indicating that the hydrocarbon-bearing types of the strata in the T32 and T33 members are mainly tight oil and gas reservoirs. At the same time, the accumulation of tight reservoirs in this area is directly related to the lateral and vertical sealing capacity of faults [17]. The upper member of the Pinghu Formation has a large sand-formation ratio, and large sets of sandstones are connected laterally, so oil and gas are easy to dissipate, and traps are not easily formed; however, the sand-formation ratio of the lower member is about 20%, which is easy to form fault-block oil and gas reservoirs (Figure 13). A small fault displacement is conducive to the vertical sealing of fault-block oil and gas reservoirs, while a large one is conducive to the lateral sealing of fault-block oil and gas reservoirs. The fault-block oil and gas reservoirs in the Pingbei area mainly rely on faults with a fault displacement greater than 30 ms to accumulate. The accumulation of oil and gas reservoirs in a few fault blocks in the south is related to the faults with a fault displacement of 0-30 ms. This shows that large fault displacements are more likely to be laterally plugged to form fault-block oil and gas reservoirs. Moreover, because the accumulation of such traps is related to large faults, they often have sufficient sources of oil and gas. The top surface of its oil and gas reservoirs often has abnormally high-pressure interfaces, which can also be used as a way to find such tight traps.

6. Conclusions

Combining three-dimensional seismic data, logging data, and source rock geochemical pyrolysis experiments of source rock in the study area, the author analyzed the distribution of coal-measure source rock and sedimentary facies evolution in the Pinghu Tectonic Belt of Xihu Sag. We have the following conclusions by research results and analysis:

(1) The coal-measure source rock of Pinghu Formation is the main source rock in the Xihu Sag, with high content of organic matter, high maturity, great potential of hydrocarbon generation, and potential for exploration and development of coalbed methane and shale oil and gas. The development and preservation of coal-measure source rock are mainly affected by the depth of water environment, so its distribution law is controlled by terrain, hanging wall and footwall of faults, and sedimentary environment

(2) The sedimentary facies of the Pinghu Tectonic Belt are dominated by wave-controlled delta facies, and river-controlled marine-land transition facies are rare. During the depositional period from the T34 member to the T31 member, there were two stages of regression and one stage of transgression. The sedimentary subfacies experienced four stages: delta front-pre-delta-neritic subfacies, underwater delta plain subfacies, delta front-neritic subfacies, and delta plain subfacies

(3) The accumulation of coalbed methane in the Pinghu Tectonic Belt is controlled by the factors of structure and burial depth, and its sag structure and higher maturity of thermal evolution are conducive to the generation and preservation of coalbed methane. Shale gas develops fractured reservoirs that are more conducive to the preservation of shale gas due to marine-continental transition facies and deposition factors of marine shale. The development of tight reservoirs is affected by wave-controlled and tide-controlled deltas, and the sandstone has good physical properties. Under the diagenesis including cementation, compaction, and dissolution, the filling and reconstruction of pores, cavities, and fractures can be ensured, so that the porosity of the reservoir is basically maintained at about 5%-15%. Under the action of oil and gas transportation and sealing by large and small faults, tight reservoirs can form a type of accumulation mainly composed of fault-block traps and supplemented by lithologic traps

Data Availability

The seismic data, logging data, and organic geochemical experimental data used to support the results of this study are included in the article.

Conflicts of Interest

The authors declare that there is no conflict of interest regarding the publication of this paper.

Acknowledgments

The research described in this paper was financially supported by the Northwest University Transverse Project Fund (no. 34000000-19-ZC0613-0011).

References

[1] G. X. Li and R. L. Zhu, "Development status, challenges and concerns of PetroChina's unconventional oil and gas," *China Petroleum Exploration*, vol. 25, no. 2, 2020.

[2] Q. M. Liu, H. F. Tang, Z. K. Lu, Z. L. Wang, N. H. Fu, and Z. Guo, "Study on choke zone configuration of braided river tight sandstone gas reservoirs: taking the tight sandstone gas reservoir of the 8th member of the middle Permian in Sulige gas field as an example," *Natural Gas Industry*, vol. 38, no. 7, pp. 25–33, 2018.

[3] Y. Q. Qu, W. Sun, D. R. Tao, B. Luo, L. Chen, and D. Z. Ren, "Pore-throat structure and fractal characteristics of tight sandstones in Yanchang Formation, Ordos Basin," *Marine and Petroleum Geology*, vol. 120, p. 104573, 2020.

[4] M. Meng, H. Ge, Y. Shen, and L. Wang, "Influence of rock fabric on salt ion diffusion behavior in upper cretaceous lacustrine shale from Songliao Basin," *Journal of Petroleum Science and Engineering*, vol. 208, p. 109355, 2022.

[5] H. X. Huang, R. X. Li, W. T. Chen et al., "Revisiting movable fluid space in tight fine-grained reservoirs: a case study from Shahejie shale in the Bohai Bay Basin, NE China," *Journal of Petroleum Science & Engineering*, vol. 207, article 109170, 2021.

[6] Y. Q. Qu, W. Sun, S. Guo, S. Shao, and X. X. Lv, "A gas-content calculation model for terrestrial shales in the Kuqa Depression, the Tarim Basin, Western China," *Interpretation-A Journal of Subsurface Characterization*, vol. 7, no. 2, pp. T513–T524, 2019.

[7] F. L. Yang, X. Xu, W. F. Zhao, and Z. Sun, "Petroleum accumulations and inversion structures in the Xihu depression, East China Sea Basin," *Journal of Petroleum Geology*, vol. 34, no. 4, pp. 429–440, 2011.

[8] F. H. Xu, G. S. Xu, Y. Liu, W. Zhang, H. Y. Cui, and Y. R. Wang, "Factors controlling the development of tight sandstone reservoirs in the Huagang Formation of the central inverted structural belt in Xihu sag, East China Sea Basin," *Petroleum Exploration and Development*, vol. 47, no. 1, pp. 101–113, 2020.

[9] A. Su, H. H. Chen, X. Chen et al., "The characteristics of low permeability reservoirs, gas origin, generation and charge in the central and western Xihu depression, East China Sea Basin," *Journal of Natural Gas Science and Engineering*, vol. 53, pp. 94–109, 2018.

[10] A. Su, H. H. Chen, M. Z. Lei, Q. Li, and C. W. Wang, "Paleopressure evolution and its origin in the Pinghu slope belt of the Xihu Depression, East China Sea Basin," *Marine and Petroleum Geology*, vol. 107, pp. 198–213, 2019.

[11] F. Liu, S. W. Huang, P. C. Yang, and C. Y. Zhang, "Characteristics of gas reservoir and controlling factors for gas accumulation in the Huagang Formation in Y structure, Xihu Sag," *Marin Geology & Quaternary Geology*, vol. 41, no. 6, pp. 174–182, 2021.

[12] P. C. Yang, F. Liu, S. Shen, J. W. Dong, and Y. H. Bai, "A study on the hydrocarbon generation potential of the coal-bearing source rocks in the Pinghu Formation of Pingbei area, the Xihu depression," *Marine Geology & Quaternary Geology*, vol. 40, no. 4, pp. 139–147, 2020.

[13] R. H. P. S. J. Yan, J. Wang, S. Y. Su, F. Zhou, and Q. L. Chen, "Discussion on the development and distribution of coal seam and dark mud shale in the west slope of Xihu depression," *Journal of Northwest University (Natural Science Edition)*, vol. 51, no. 3, pp. 447–458, 2021.

[14] M. Meng, H. Ge, Y. Shen, and W. Ji, "Evaluation of the pore structure variation during hydraulic fracturing in marine shale reservoirs," *Journal of Energy Resources Technology*, vol. 143, no. 8, 2021.

[15] S. H. Jiang, S. Z. Li, X. G. Chen, H. X. Zhang, and G. Wang, "Simulation of oil–gas migration and accumulation in the East China Sea Continental Shelf Basin: a case study from the Xihu Depression," *Geological Journal*, vol. 51, no. 51, pp. 229–243, 2016.

[16] M. X. Du and Z. Z. Xu, "Geological characteristics and development potential of deep gas reservoirs in H oil and gas field in Xihu Sag," *China Offshore Oil and Gas*, vol. 2, 2013.

[17] D. H. Jiang, R. H. Pu, S. Y. Su, C. Y. Fan, F. Zhou, and P. C. Yang, "Accumulation conditions of large-scale oil and gas fields in the slope zone of faulted basins-Pingbei gentle slope faults and favorable lithological reservoir control areas in Xihu Sag," *Natural Gas Industry*, vol. 41, no. 11, pp. 33–42, 2021.

[18] M. D. Burnett, J. P. Castagna, E. Méndez-Hernández et al., "Application of spectral decomposition to gas basins in Mexico," *The Leading Edge*, vol. 22, no. 11, pp. 1130–1134, 2003.

[19] J. P. Castagna, S. J. Sun, and R. M. Siegfried, "Instantaneous spectral analysis: detection of low-frequency shadows associated with hydrocarbons," *The Leading Edge*, vol. 22, no. 2, pp. 120–127, 2003.

[20] A. Nikoo, A. R. Kahoo, H. Hassanpour, and H. Saadatnia, "Using a time-frequency distribution to identify buried channels in reflection seismic data," *Digital Signal Processing*, vol. 54, pp. 54–63, 2016.

[21] G. Gang, W. Z. Gang, G. C. Zhang, and W. J. He, "Geological features and gas accumulation simulation experiments of the Liwan 3-1 gas field in the Baiyun Sag, Pearl River Mouth Basin," *Natural Gas Industry*, vol. 34, pp. 26–35, 2014.

[22] X. C. Wu, R. H. Pu, and H. Y. Xue, "Detection and analysis to gas-bearing of seafloor fans in the Zhuhai Formation of the Jieyang sag, Pearl River Mouth Basin," *Chinese Journal of Geophysics*, vol. 62, pp. 2732–2747, 2019.

[23] T. W. C. Hilde, S. Uyeda, and L. Kroenke, "Evolution of the western pacific and its margin," *Tectonophysics*, vol. 38, no. 1-2, pp. 145–165, 1977.

[24] L. W. Hao, Q. Wang, H. F. Tao, X. Li, D. Ma, and H. Ji, "Geochemistry of Oligocene Huagang Formation clastic rocks, Xihu Sag, the East China Sea Shelf Basin: provenance, source

weathering, and tectonic setting," *Geological Journal*, vol. 53, no. 1, pp. 397–411, 2018.

[25] J. R. Ye, H. R. Qing, S. L. Bend, and H. R. Gu, "Petroleum systems in the offshore Xihu Basin on the continental shelf of the East China Sea," *AAPG Bulletin*, vol. 91, no. 8, pp. 1167–1188, 2007.

[26] W. Yang, Y. Qin, Y. Liu, S. M. Liu, D. Elsworth, and R. Zhang, "Organic geochemical and petrographic characteristics of the coal measure source rocks of Pinghu Formation in the Xihu Sag of the East China Sea Shelf Basin: implications for coal measure gas potential," *Acta Geologica Sinica*, vol. 94, no. 2, pp. 364–375, 2020.

[27] P. C. H. Veeken and M. B. Van, *Seismic Stratigraphy and Depositional Facies Models*, EAGE Publications, Houten, 2013.

[28] A. El-Sorogy, K. Al-Kahtany, S. Almadani, and M. Tawfik, "Depositional architecture and sequence stratigraphy of the Upper Jurassic Hanifa Formation, central Saudi Arabia," *Journal of African Earth Sciences*, vol. 139, pp. 367–378, 2018.

[29] P. C. Scruton, *Delta Building and the Deltaic Sequence*, Recent Sediments Northwest Gulf of Mexico, 1960.

[30] W. Fisher and J. Mcgowen, "Depositional systems in Wilcox Group (Eocene) of Texas and their relation to occurrence of oil and gas," *AAPG Bulletin*, vol. 53, no. 1, pp. 30–54, 1969.

[31] J. Y. Zhang, Y. C. Lu, W. Krijgsman, J. S. Liu, X. Q. Li, and X. B. Du, "Source to sink transport in the Oligocene Huagang Formation of the Xihu Depression, East China Sea Shelf Basin," *Marine and Petroleum Geology*, vol. 98, pp. 733–745, 2018.

[32] Q. Zhao, H. T. Zhu, X. H. Zhou, Q. H. Liu, H. Cai, and W. Z. Gao, "Continental margin sediment dispersal under geomorphic control in Xihu Depression, East China Sea Shelf Basin," *Journal of Petroleum Science and Engineering*, vol. 205, p. 108738, 2021.

[33] S. C. Zhang, B. M. Zhang, and L. Z. Bian, "Development constraints of marine source rocks in China," *Earth Science Frontiers*, vol. 12, no. 3, pp. 39–48, 2005.

[34] D. G. Liang, T. L. Guo, and L. Z. Bian, "Some progresses on studies of hydrocarbon generations and accumulation in marine sedimentary regions, southern China (part 3): controlling factors on the sedimentary facies and development of Palaeozoic marine source rocks," *Marine Origin Petroleum Geology*, vol. 14, no. 2, pp. 1–19, 2009.

[35] F. W. Wang, D. X. Chen, Q. C. Wang, W. L. Du, and S. Y. Chang, "Quantitative evaluation of caprock sealing controlled by fault activity and hydrocarbon accumulation response: K gasfield in the Xihu Depression, East China Sea Basin," *Marine and Petroleum Geology*, vol. 134, article 105352, 2021.

[36] M. D. Zuber, "Production characteristics and reservoir analysis of coalbed methane reservoirs," *International Journal of Coal Geology*, vol. 38, no. 1-2, pp. 27–45, 1998.

[37] M. Pillalamarry, S. Harpalani, and S. M. Liu, "Gas diffusion behavior of coal and its impact on production from coalbed methane reservoirs," *International Journal of Coal Geology*, vol. 86, no. 4, pp. 342–348, 2011.

[38] Y. Qin, T. A. Moore, J. Shen, Z. B. Yang, Y. L. Shen, and G. Wang, "Resources and geology of coalbed methane in China: a review," *International Geology Review*, vol. 60, no. 5-6, pp. 777–812, 2018.

[39] R. Thiery, J. Pironon, F. Walgenwitz, and F. Montel, "Individual characterization of petroleum fluid inclusions (composition and P - T trapping conditions) by microthermometry and confocal laser scanning microscopy: inferences from applied thermodynamics of oils," *Marine and Petroleum Geology*, vol. 19, no. 7, pp. 847–859, 2002.

[40] J. S. Liu, S. L. Kang, W. C. Shen et al., "Petrology and hydrocarbon significance of the coaly source rocks from the Pinghu Formation in the Xihu Sag, East China Sea Shelf Basin," *Energy Exploration & Exploitation*, vol. 38, no. 5, pp. 1295–1319, 2020.

[41] X. H. Zhou, G. S. Xu, H. Y. Cui, and W. Zhang, "Fracture development and hydrocarbon accumulation in tight sandstone reservoirs of the Paleogene Huagang Formation in the central reversal tectonic belt of the Xihu Sag, East China Sea," *Petroleum Exploration and Development*, vol. 47, no. 3, pp. 499–512, 2020.

[42] W. G. Wang, C. Y. Lin, X. G. Zhang, C. M. Dong, L. H. Ren, and J. L. Lin, "Effect of burial history on diagenetic and reservoir-forming process of the Oligocene sandstone in Xihu sag, East China Sea Basin," *Marine and Petroleum Geology*, vol. 112, p. 104034, 2020.

[43] W. G. Wang, C. Y. Lin, X. G. Zhang, C. M. Dong, L. H. Ren, and J. L. Lin, "Structural controls on sandstone compaction within the anticline crest and flank: an example from the Xihu Sag, East China Sea Basin," *Journal of Petroleum Science and Engineering*, vol. 211, article 110157, 2022.

[44] Y. J. Jiang, J. Zhou, X. F. Fu, L. K. Cui, C. Fang, and J. M. Cui, "Analyzing the origin of low resistivity in gas-bearing tight sandstone reservoir," *Geofluids*, vol. 2021, Article ID 4341804, 15 pages, 2021.

[45] W. G. Wang, C. Y. Lin, J. L. Lin, X. G. Zhang, C. M. Dong, and L. H. Ren, "Three-dimensional mechanical compaction and chemical compaction simulation of the Oligocene sandstone in Xihu sag, East China Sea Basin," in *Unconventional Resources Technology Conference, Virtual*, pp. 1640–1659, 2020.

[46] S. J. Zhao, Q. Fu, and W. R. Ma, "Pore-throat size distribution and classification of the Paleogene tight sandstone in Lishui sag, East China Sea Shelf Basin, China," *Energy & Fuels*, vol. 35, no. 1, pp. 290–305, 2021.